

¹ Benazir Meerasha² Martin Sagayam

A Comparison of Pixel Based and Object Based Image Classification for Cropland Area Estimation



Abstract: - Pixel-based (PB) and object-based (OB) Land Use–Land Cover (LULC) classification techniques can be applied in Google Earth Engine (GEE), a flexible cloud-based platform, because of its numerous state-of-the-art functions that comprise several Machine Learning (ML) methods. Adding some texture measure, any measure to a classification usually improves the accuracy. Object segmentation and object textural analysis are two OB methods that are still uncommon in the GEE environment. Object based image classification is difficult because it can be challenging to concatenate the correct functions and adjust various parameters in order to get past the computational limitations of GEE. The goal of this work is to develop and test an OB classification approach that combines the ML algorithm Random Forest (RF) to perform the final classification, the Gray-Level Co-occurrence Matrix (GLCM) to calculate cluster textural indices and the Simple Non-Iterative Clustering (SNIC) algorithm to identify spatial clusters. The primary seven GLCM indices are subjected to a Principal Components Analysis (PCA) in order to combine the textural data needed for the OB classification into a single band. The proposed methodology was broadly tested in a 304 km² study area, located in the Telangana state (India), using Sentinel 2 (S2).

Keywords: Google Earth Engine (GEE), Sentinel 2, SNIC, GLCM, machine learning, Random Forest (RF).

I. INTRODUCTION

In the last decade, remote sensing data processing shifted to cloud-based platforms like Google Earth Engine, streamlining large-scale geospatial analysis [1]. Remote sensing applications, such as producing Land Use/Land Cover maps, reveal human land use and Earth surface characteristics. Google Earth Engine streamlines creating cloud-free, multi-temporal composite datasets for landscape analysis and change detection [2]. Conventional Land Use/Land Cover (LULC) classification in remote sensing relies on spectral signatures and pixel-based discrimination using training data. Recent advancements in image segmentation, particularly Geographic Object-Based Image Analysis (GEOBIA), offer enhanced capabilities for delineating and classifying landscape objects or patches at various scales [3]. The spatial relationship between pixels is taken into account when analyzing texture using the Gray-Level Co-occurrence Matrix (GLCM), a statistical technique. It functions by examining pixel combinations and determining the probability with which various pixel brightness value combinations (also known as gray levels) occur in an image. GLCM is a tool that Google Earth Engine users may use to extract texture information from satellite images. This information is useful for a variety of applications, including environmental monitoring, urban planning, and land cover classification. Google Earth Engine's function determines texture measurements for each pixel in the input image using GLCM. Texture information can be incorporated into the classification process using GLCM, which is especially helpful for differentiating between land cover types with similar spectral signatures but distinct spatial patterns. With its versatility, GLCM may be used with a wide range of remote sensing data types from GEE, including Sentinel, Landsat, and other sources. Large datasets can be processed by Google Earth Engine's robust computational capabilities, which makes it possible to analyze GLCM features over wide geographic regions. Without the requirement for powerful computing resources, Google Earth Engine offers an approachable framework for GLCM and other sophisticated image processing algorithms to be implemented. Google Earth Engine's cloud-based architecture saves time and local storage by processing GLCM and other computations efficiently. These benefits give GLCM a more comprehensive understanding of land cover and land use patterns, making it a useful supplement to pixel-based classification methods in Google Earth Engine.

II. LITERATURE REVIEW

Object-based (OB) methods excel with higher-resolution data, despite increased computational costs, while pixel-based (PB) approaches suit lower resolutions but may show a "salt-pepper" effect. Object delineation involves clustering and segmentation, with the Simple Non-Iterative Clustering (SNIC) algorithm in GEE

¹ Research Scholar, Electronics and Communication Engineering Department, Karunya Institute of Technology and Sciences, India.
Email: benazirm@karunya.edu.in

² Assistant Professor, Electronics and Communication Engineering Department, Karunya Institute of Technology and Sciences, India.
Email: martinsagayam@karunya.edu

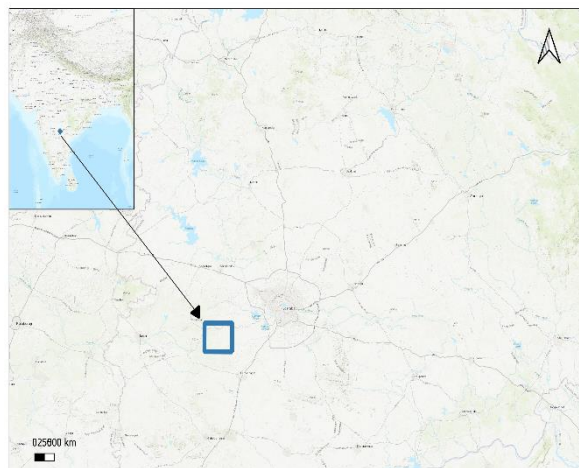
Copyright © JES 2024 on-line: journal.esrgroups.org

proving efficient. GEOBIA combines spectral, spatial, texture, and context information for the final object classification. GEE's Gray-Level Co-occurrence Matrix (GLCM) enables effective textural index extraction from greyscale images, allowing GEOBIA application even on greyscale images. Principal Component Analysis aids in reducing GLCM output dimensionality [4]. Both pixel-based (PB) and object-based (OB) classification processes offer diverse methods. Modern Machine Learning (ML) classifiers, like CART, RF and SVM outperform traditional ones, providing accurate LULC results [5]. Object based image analysis encompassing object segmentation and textural analysis, is not yet widely adopted in GEE, likely due to challenges in combining functions and overcoming computational limits. The SNIC algorithm is extensively utilized in GEE for spatial cluster identification, enhancing LULC classification. For instance, Mahdianpari et al. employed SNIC and Random Forest in GEE for object-based classification in producing the Canadian Wetland Inventory, significantly improving upon pixel-based classification [6]. In certain GEE-based studies, segmentation steps were conducted externally. Stromann et al. [7] utilized commercial software for object-based LULC SVM classification, integrating S1 and S2 data, followed by feature characterization in GEE based on GLCM. Xiong et al. [8], [9] generated a 30-m cropland map for Africa using PB and OB algorithms, S2, and L8 data, employing SVM and Random Forest. The segmentation step involved recursive hierarchical segmentation on a NASA Pleiades supercomputer. GLCM in GEE was used by Godinho et al. [9] to enhance LULC classification by combining multispectral bands, vegetation indices, and GLCM textures. Mananze et al. [10] derived a Land Cover map in Mozambique using Landsat 7 and 8 bands, vegetation indices and GLCM-derived textural features. In Sumatra and Indonesia, synthetic aperture radar and optical imagery were fused to map oil palm plantations using GLCM textural features from Synthetic Aperture Radar (SAR) data, improving classification accuracy [11]. This work intends to design and assess an object-based (OB) classification technique that employs widely used machine learning algorithms RF for final classification, the SNIC algorithm for spatial cluster identification, and GLCM for cluster textural indices. The method is incorporated into an easy-to-use GEE code that is openly accessible for parameter adjustment and comparison with pixel-based (PB) methods. Confusion matrices, which include producer, user, and total accuracy are used to evaluate accuracy visually.

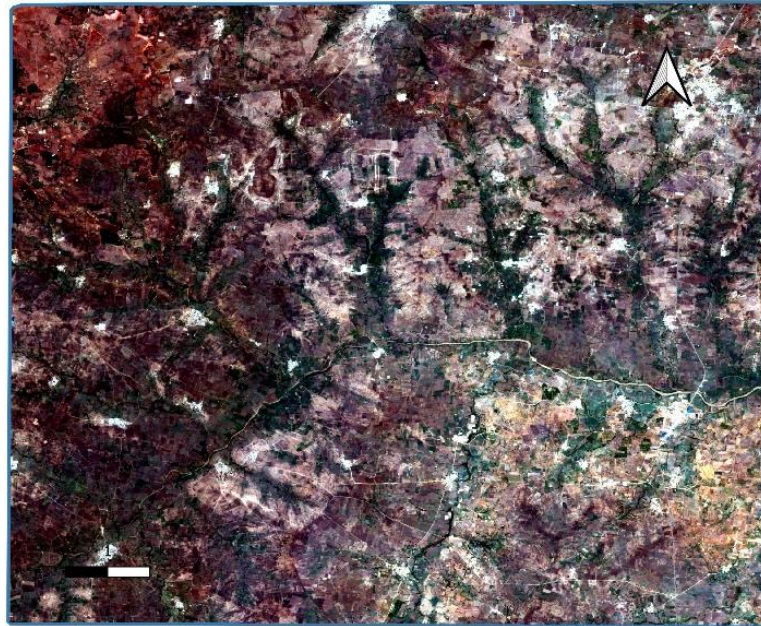
III. MATERIALS AND METHODS

3.1 Study Area

The study area is located in southern Indian state of Telangana, covering area of 308.304 Sq.km (Figure.1). The latitude and longitude of the study area is (17.32,77.99). The study area is gently undulating with elevation ranging from 520 m to 730 m above Mean Sea Level. The elevation is high in western part of the study area and slowly decreases towards the eastern part. The average rainfall of the study area is 875 mm/year with the highest being in NW portion of the watershed recorded higher rainfall (~ 1000 mm) in comparison to SE which receives 700 mm. The majority of the area covered by Pediplain pediment complex of denudational origin covering 85% of study area makes this terrain more suitable for agricultural activity. Specifically, the western portion of the area is well-suited for growing cotton crops due to the presence of Deccan traps. The prevalence of loamy soil in the western region compared to the eastern region makes it more conducive to agricultural activity, resulting in the majority of the double crop regions being located in the western part of the study area. The majority areas are rain-fed region and cultivated with cotton, maize and vegetables.



(a)



(b)

Figure 1. Study area location in Telangana, India (a). RGB image based on 10 m resolution Sentinel 2 bands (b).

3.2 Training and Validation Sample Data

Five LULC classes make up the intricate landscape mosaic that is present in the study area: (1) water- bodies of water (2) cropland- permanent crops (3) urban- built up areas (4) trees-forests, such as those that grow alongside rivers or lakes, and other tiny, sparsely vegetated landscapes; (5) agriculture- vegetables and cereals. Using a visual interpretation of the identical base layers, 300 validation points in total were created at random and manually labeled (Table 1). In the literature, this strategy is frequently employed [12].

Table I: The number of validation points for each Land Use–Land Cover (LULC) class

Class	Number of validation points
Water	30
Cropland	80
Urban	70
Tree	50
Agriculture	70
Total	300

IV. METHODOLOGY

In a unified Google Earth Engine workflow, create an initial dataset, classify land cover using Pixel-Based and Object-Oriented techniques with RF in separate scripts for efficiency, and assess accuracy through confusion matrices.

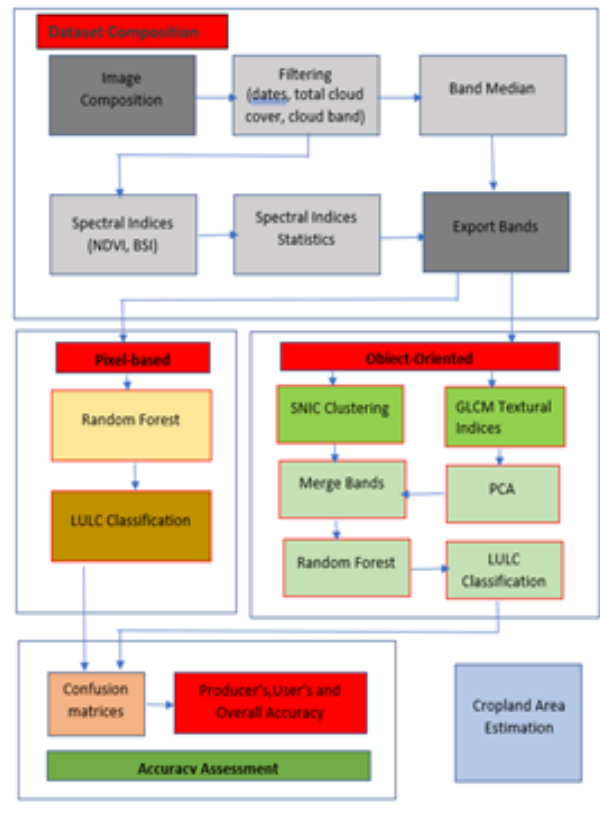


Figure 2. The methodological workflow implemented in Google Earth Engine (GEE).

The proposed technique was fully analyzed using Sentinel 2 satellite data and validated using RF classifiers with various input settings. The optimal pairings were identified by visual comparison, assessment based on area percentage and categorization accuracy, and selection based on overall accuracy.

4.1 Data Composition

Creating the foundational dataset is crucial for the categorization of land use/land cover (LULC). The method computes the NDVI and BSI for better classification accuracy, filters and cloud-masks Sentinel 2 (S2) data in Google Earth Engine (GEE), and uses data augmentation to handle seasonal volatility. The procedure generates a composite dataset containing the primary statistics and median pixel values of the selected spectral indices prior to exporting the necessary bands [13].

The following input criteria must be supplied in order for the code to run:

- region of interest (roi), a polygon used to define the research area
- period of interest, which is determined by defining the start and end dates (MM-DD-YYYY)
- the input bands, which are chosen from the accessible S2 bands

The completed dataset's output bands are called outBands. They are chosen from the mean, maximum, and standard deviation of the NDVI, the median of the inBands and the BSI indexes. The code starts by using cloud masking for Sentinel 2 to collect images with a 10 percent cloud cover limitation throughout the course of a year, from March 1, 2020, to March 31, 2021. (S2). Band selection, median composite, NDVI and BSI composite, and export of selected bands for the original S2 dataset are applied to the final image collections.

V. RESULTS

5.1 LULC Classification

The input requirements for LULC classification in GEE utilizing PB and OO techniques with an RF classifier are labeled training data and images [14]

- roi: region of interest;
- gcp: a collection of features consists of all training data labeled with codes corresponding to LULC classes;

- valgcp: validation points randomly generated and labeled manually with the LULC code used to assess the model's accuracy;
- dataset: generated in the "Dataset composition" step.

The training data consists of feature collections with a 10 m buffer between each point that represent LULC classes and are generated using GEE. The accuracy evaluation process makes use of validation points. Using pre-existing datasets, the code conducts PB and OB LULC classifications. With 50 trees in the image, the RF classifier quickly classifies the image in the PB classification stage. A final morphological operation is applied to the output classification in order to clean up all of the output and lessen the "salt and pepper" impact.

Spatial clustering, textural index computation, and final classification are steps in the OB classification process. It applies the SNIC and GLCM algorithms in a two-step manner. SNIC employs a seed grid to generate clusters on PB categorization bands. Tests are conducted to determine the ideal values of seed spacing. By creating clusters, SNIC creates a multi-band raster that includes average feature values and cluster information. In GEE, SNIC parameters such as "compactness factor" for cluster shape, "connectivity" (4 or 8) for merging, and "neighborhoodSize" to prevent artifacts were set as follows: compactness = 0, connectivity = 8, and neighborhood size = 256. Since SNIC outputs vary depending on visualization scale, the code sets a proper output scale using "reproject" ($S_2 = 10$). GLCM requires an 8-bit grey-level image, which is generated by combining NIR, Red, and Green bands. PCA is applied to 7 selected GLCM metrics after standardization, resulting in a representative first PC. Each SNIC cluster's PC1 average is added to the segmentation results of SNIC. Pixel-based RF training is replicated in OB LULC classification. Pixel count per class determines total area (hectares), with all operations optimized in the raster domain for code efficiency.

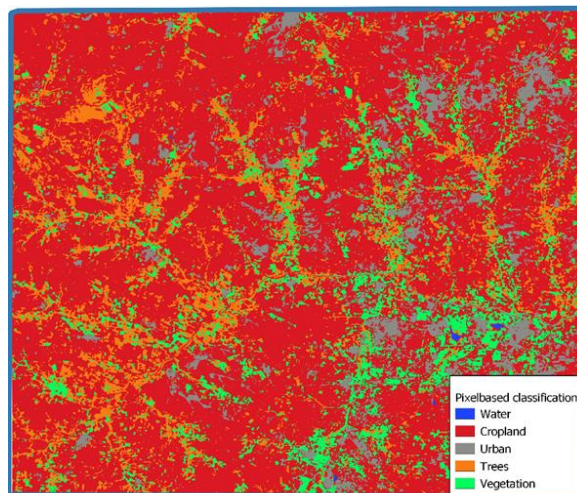


Figure 3. Pixel based LULC classification.

Fig 3 presents the outcomes of the OA tests that were carried out in the research region. With the S2 data, the OB approach, and the inclusion of the GLCM textural information produces more accurate OA (97%). The OB technique produces superior results on the higher spatial resolution datasets, while the OB approach outperforms the PB approach on S2 data. Although the rise in OA is more noticeable for the S2 dataset, the addition of the textural information enhances the OB categorization for the S2 datasets. An intriguing part of the research area distinguished by the presence of the main metropolitan center, a segment of waterbody, and the nearby multicultural area illustrates the differences between the selected categories, also with regard to cluster size. Fig 3 represents each class's proportion of the total area filled by the chosen categorization procedures.

There are notable differences between the outcomes of the different classification systems in the Land cover maps and associated areas of Land cover classes. In comparison to the S2 OB classification, the primary differences are shown in cropland and agriculture. However, given their limited area coverage, there is also a noteworthy divergence seen in built-up areas, trees, and waterbodies. The S2 classification correctly predicts built-up regions in particular. When it comes to their overall extent, trees and agriculture seem more alike than the pixel-based classification. In OB classification agricultural land is classified very clearly and noteworthy difference seen between trees, agriculture and cropland. On the other hand, the PB outputs show a very irregular spatial arrangement of trees, agriculture, and cropland when comparing the LULC maps with the OB S2 result (Fig 3).

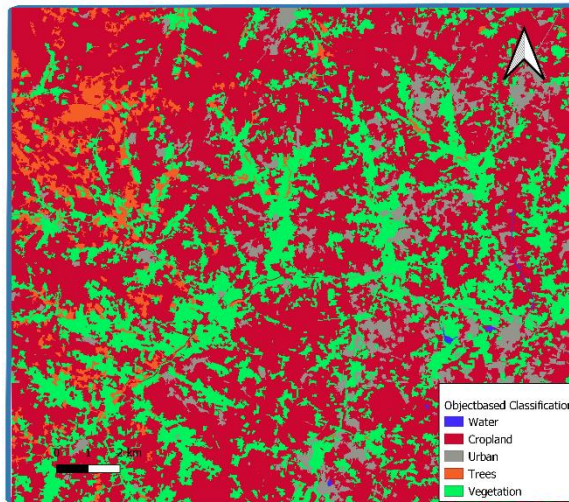


Figure 4. Object oriented LULC classification

As part of the accuracy evaluation procedure, LULC from validation points and classification outputs are compared in GEE using a confusion matrix.

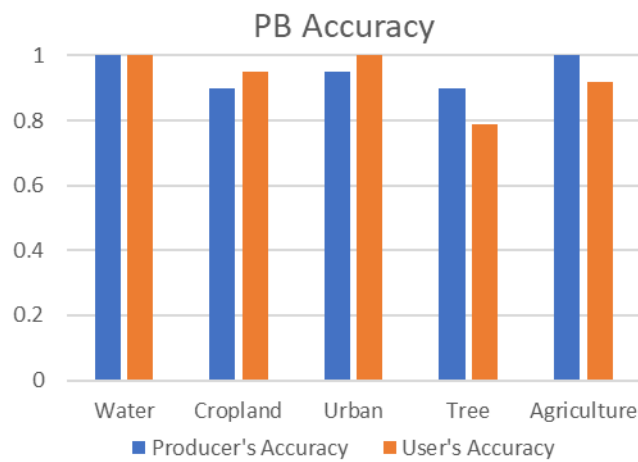


Figure 5. Pixel based Producers and Users Accuracy.

The users and producers accuracy for PB classification for the class water is same. The producers and users accuracy for OB classification for the class water is also same. In PB classification the producers and users accuracy for cropland is 0.8 and 0.85 whereas in OB classification the producers and users accuracy is 0.9 and 1. The producers and users accuracy for the class urban and tree in OB classification is 1 whereas for the class agriculture it is 1 and 0.83.

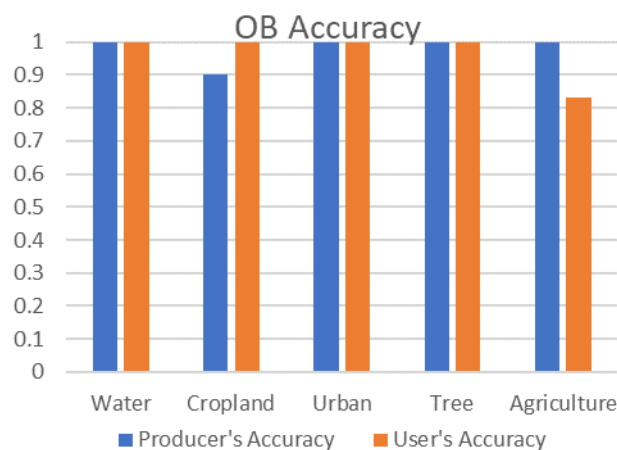


Figure 6. Object based Producers and Users Accuracy.

The producers and users accuracy for the class tree in PB classification is 0.8 and 0.79 whereas for the class agriculture it is 1 and 0.92. The calculation of Overall Accuracy (OA), Kappa statistics (K), Users Accuracy (UA), and Producers Accuracy (PA) creates the confusion zones (omission and commission errors). The accuracy of the findings indicates their proximity to reality, while the Kappa value indicates the degree of error reduction in comparison to random categorization. Due to problems interpreting Kappa coefficients, OA, PA and UA are the main topics of this study. Numerous factors, such as class selection, point distribution, and satellite data attributes, might affect accuracy. The algorithm compares and assesses each categorization using established methods. The general precision of categorization is based on pixels.

VI. DISCUSSION

The development of new earth observation satellites, improvements in sensor resolutions, the availability of large public datasets and rising computing power are all contributing to the growth of the remote sensing field. A key open-source cloud platform for worldwide geospatial research and simulation is Google Earth Engine (GEE). Its extensive database of easily accessed data allows users to participate in a variety of applications, which greatly adds to its success on a large scale. One noteworthy development in the subject is the ongoing evolution of geospatial object-based analysis (GEOBIA) approaches, especially when combined with machine learning (ML) algorithms. Overall, GEE's accessibility and functionality underscore its significance in advancing remote sensing capabilities and driving innovation in geospatial analysis. This study highlights the utility of GEE as it simplifies complex image processing tasks and facilitates the creation of multi-temporal composite images. By utilizing GEE's capabilities, researchers can streamline sophisticated geospatial analyses with relative ease. The findings highlight GEE's role as a versatile platform, empowering users to explore various aspects of remote sensing and contributing to advancements in the field.

The research established an object-based framework that combines machine learning (ML), GLCM, and SNIC algorithms into a publicly available GEE code. The same input bands and classification algorithm can be used in a pixel-based (PB) approach, and users can compare the outcomes by changing the parameters in this annotated method. Users can examine producer and user accuracies for each classes as well as overall accuracy by visually inspecting LULC maps and going over accuracy matrices. These metrics offer more precise data regarding the dependability of the classification process and probable value addition. This strategy ensures flexibility and ease of comparison by making it easy for users to navigate and adjust parameters. The significance of visual inspection and accuracy assessment in evaluating the efficacy and resilience of land use/cover classification methods is also emphasized in this studies.

Even though the SNIC's usual application inside GEE is based on a grid of seeds that is consistently spaced, it produced the object segmentation quite successfully. Using seeds that are created by determining the local minimum or maximum of variation might be an improvement in this regard. Testing the results of different seed spacings may be quite helpful in determining the more effective cluster size while also taking the size of the landscape patches into consideration, as though this application demonstrates. The suggested method analyzed the textural aspects of the input datasets by combining SNIC and GLCM, in contrast to earlier research. An approach that is often used in image processing has demonstrated excellent performance in GEE as well.

As mentioned, all of the work computed on object recognition and the textural characterization was executed in the raster domain, where GEE performs efficiently. Despite being linked to faster code execution, this method ignores the object's geometry, which might be crucial for typical objects at higher resolutions. Object vectorization could be able to get around this restriction. However, in the context of the raster-oriented GEE environment, the few attempts have been marked by extremely slow code execution or processing blocks brought on by an excessive number of geometries.

Classifying complex Land Use Land Cover categories, such as built-up areas and perennial crops, was significantly more accurate when GLCM data was used, even though Sentinel-2 imagery had a 10-meter resolution. Challenges were given to examine the Object-based capabilities within Google Earth Engine (GEE), exhibiting exceptional accuracy. The achievement illustrates the potential of GLCM analysis and Object-based approaches when applied to Sentinel-2 data, particularly in distinguishing complicated land use and land cover patterns. The effectiveness of these techniques in capturing a variety of land cover features was proved by the identification of high-entropy built-up areas and regions with regular textures, such as perennial crops. The integration of GLCM characteristics was beneficial in differentiating between different types of land cover according to their textural characteristics. In addition, the focus of the study on testing Object-based methodologies suggests a wider interest in investigating novel strategies for accurate land cover classification. In

summary, the results highlight the encouraging potential of utilizing GLCM analysis and Object-based techniques to improve the precision of LULC classification through satellite imagery.

VII. CONCLUSION

A confusion matrix is used to compare validation points and classification results for Land Use and Land Cover (LULC) in Google Earth Engine (GEE) in order to evaluate accuracy. With indicators like Overall Accuracy (OA), Kappa statistics (K), User's Accuracy (UA), and Producer's Accuracy (PA) accounting for both omission and commission mistakes, this matrix aids in the identification of confusion zones. While the Kappa coefficient assesses error reduction in comparison to random classification, the OA measures the degree to which outcomes match the truth. Due to challenges in interpreting Kappa coefficients, this study focuses on OA, PA, and UA. The accuracy assessment can be influenced by a number of factors, including class selection, point distribution, and satellite data properties. The code incorporates standardized procedures that facilitate the evaluation and comparison of each classification; the object-oriented classification achieves an OA of 0.97, while the pixel-based classification achieves an OA of 0.90. The cropland area estimated by the study is 20,051.47 hectares. The larger study areas provide computational limitations, which will be addressed by future research and also focuses on the automatic selection of the super pixel size of SNIC. In general, complex comparison techniques are used in the accuracy assessment process to determine how reliable LULC classifications are. Through the use of many metrics and standard operating processes, researchers are able to assess classification results in an efficient manner and pinpoint areas that require improvement. The discrepancy in classification accuracy between object-oriented and pixel-based approaches highlights how crucial it is to use classification strategies that are appropriate for the goals and features of the research area.

To improve accuracy assessment methods, further research is needed, especially to handle computational difficulties that come with larger study regions. Furthermore, investigating automated methods for parameter selection might simplify the process of evaluating accuracy, making assessments in remote sensing applications more effective and trustworthy.

REFERENCES

- [1] N. Gorelick, M. Hancher, M. Dixon, S. Ilyushchenko, D. Thau, and R. Moore, 'Google Earth Engine: Planetary-scale geospatial analysis for everyone', *Remote Sens Environ*, vol. 202, pp. 18–27, Dec. 2017, doi: 10.1016/J.RSE.2017.06.031.
- [2] J. Biswas, M. A. Jobaer, S. F. Haque, M. S. Islam Shozib, and Z. A. Limon, 'Mapping and monitoring land use land cover dynamics employing Google Earth Engine and machine learning algorithms on Chattogram, Bangladesh', *Heliyon*, vol. 9, no. 11, Nov. 2023, doi: 10.1016/j.heliyon.2023.e21245.
- [3] T. Blaschke, 'Object based image analysis for remote sensing', *ISPRS Journal of Photogrammetry and Remote Sensing*, vol. 65, no. 1, pp. 2–16, Jan. 2010, doi: 10.1016/J.ISPRSJPRS.2009.06.004.
- [4] X. Zhang, M. Zeraatpisheh, M. M. Rahman, S. Wang, and M. Xu, 'Texture is important in improving the accuracy of mapping photovoltaic power plants: A case study of ningxia autonomous region, china', *Remote Sens (Basel)*, vol. 13, no. 19, Oct. 2021, doi: 10.3390/rs13193909
- [5] P. Chachondhia, A. Shakya, and G. Kumar, 'Performance evaluation of machine learning algorithms using optical and microwave data for LULC classification', *Remote Sens Appl*, vol. 23, p. 100599, Aug. 2021, doi: 10.1016/J.RSASE.2021.100599.
- [6] M. Mahdianpari et al., 'Big Data for a Big Country: The First Generation of Canadian Wetland Inventory Map at a Spatial Resolution of 10-m Using Sentinel-1 and Sentinel-2 Data on the Google Earth Engine Cloud Computing Platform', *Canadian Journal of Remote Sensing*, vol. 46, no. 1, pp. 15–33, Jan. 2020, doi: 10.1080/07038992.2019.1711366.
- [7] O. Stromann, A. Nascetti, O. Yousif, and Y. Ban, 'Dimensionality Reduction and Feature Selection for Object-Based Land Cover Classification based on Sentinel-1 and Sentinel-2 Time Series Using Google Earth Engine', *Remote Sensing 2020*, Vol. 12, Page 76, vol. 12, no. 1, p. 76, Dec. 2019, doi: 10.3390/RS12010076.
- [8] J. Xiong et al., 'Nominal 30-m Cropland Extent Map of Continental Africa by Integrating Pixel-Based and Object-Based Algorithms Using Sentinel-2 and Landsat-8 Data on Google Earth Engine', *Remote Sensing 2017*, Vol. 9, Page 1065, vol. 9, no. 10, p. 1065, Oct. 2017, doi: 10.3390/RS9101065.
- [9] S. Godinho, N. Guiomar, and A. Gil, 'Estimating tree canopy cover percentage in a mediterranean silvopastoral systems using Sentinel-2A imagery and the stochastic gradient boosting algorithm', *Int J Remote Sens*, vol. 39, no. 14, pp. 4640–4662, Jun. 2018, doi: 10.1080/01431161.2017.1399480.
- [10] S. Mananze, I. Poças, and M. Cunha, 'Mapping and Assessing the Dynamics of Shifting Agricultural Landscapes Using Google Earth Engine Cloud Computing, a Case Study in Mozambique', *Remote Sensing 2020*, Vol. 12, Page 1279, vol. 12, no. 8, p. 1279, Apr. 2020, doi: 10.3390/RS12081279.

- [11] T. Sarzynski, X. Giam, L. Carrasco, and J. S. Huay Lee, 'Combining Radar and Optical Imagery to Map Oil Palm Plantations in Sumatra, Indonesia, Using the Google Earth Engine', *Remote Sensing* 2020, Vol. 12, Page 1220, vol. 12, no. 7, p. 1220, Apr. 2020, doi: 10.3390/RS12071220.
- [12] A. Whyte, K. P. Ferentinos, and G. P. Petropoulos, 'A new synergistic approach for monitoring wetlands using Sentinels -1 and 2 data with object-based machine learning algorithms', *Environmental Modelling & Software*, vol. 104, pp. 40–54, Jun. 2018, doi: 10.1016/J.ENVSOFT.2018.01.023.
- [13] R. P. Singh, N. Singh, S. Singh, and S. Mukherjee, 'Normalized Difference Vegetation Index (NDVI) Based Classification to Assess the Change in Land Use/Land Cover (LULC) in Lower Assam, India', *International Journal of Advanced Remote Sensing and GIS*, vol. 5, no. 1, pp. 1963–1970, Oct. 2016, doi: 10.23953/CLOUD.IJARSG.74.
- [14] C. Champagne, H. McNairn, B. Daneshfar, and J. Shang, 'A bootstrap method for assessing classification accuracy and confidence for agricultural land use mapping in Canada', *International Journal of Applied Earth Observation and Geoinformation*, vol. 29, no. 1, pp. 44–52, Jun. 2014, doi: 10.1016/J.JAG.2013.12.016.